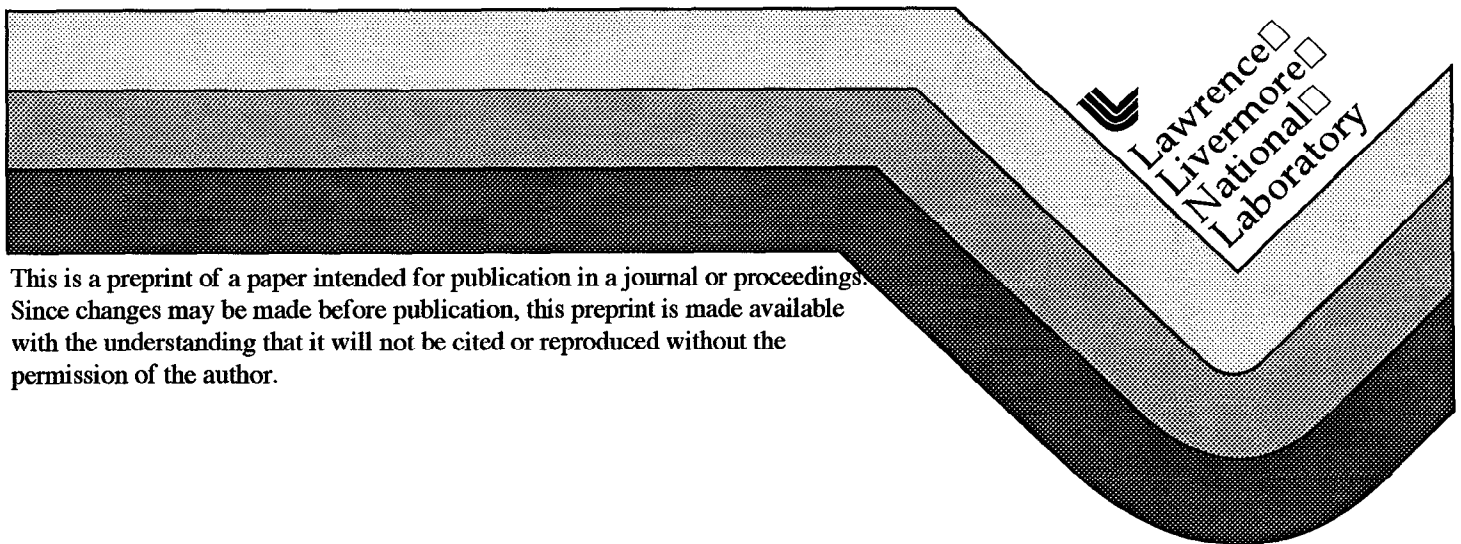


Equation of State of Insensitive High Explosives

F. H. Ree
J. A. Viecelli
M. V. Thiel

This paper was prepared for submittal to
11th International Detonation Symposium
Snowmass Village, CO
August 31-September 4, 1998

August 12, 1998



This is a preprint of a paper intended for publication in a journal or proceedings. Since changes may be made before publication, this preprint is made available with the understanding that it will not be cited or reproduced without the permission of the author.

DISCLAIMER

This document was prepared as an account of work sponsored by an agency of the United States Government. Neither the United States Government nor the University of California nor any of their employees, makes any warranty, express or implied, or assumes any legal liability or responsibility for the accuracy, completeness, or usefulness of any information, apparatus, product, or process disclosed, or represents that its use would not infringe privately owned rights. Reference herein to any specific commercial product, process, or service by trade name, trademark, manufacturer, or otherwise, does not necessarily constitute or imply its endorsement, recommendation, or favoring by the United States Government or the University of California. The views and opinions of authors expressed herein do not necessarily state or reflect those of the United States Government or the University of California, and shall not be used for advertising or product endorsement purposes.

EQUATION OF STATE OF INSENSITIVE HIGH EXPLOSIVES

Francis H. Ree, James A. Viccelli, and Mat van Thiel
Lawrence Livermore National Laboratory
P. O. Box 808, Livermore, CA 94550

Detonation of an insensitive high explosive formulated with a fluorine containing binder produces a large amount of condensed carbon and gaseous HF product, which transforms into CF_4 as the pressure is increased. The former (carbon condensation) is characterized by slow energy release, while the latter (HF) has no shockwave data. We have identified that these two items are the key factors, which make reliable prediction of the performance of an insensitive high explosive very difficult. This paper describes physical models to address these issues and apply the models to analyze experimental data of LX-17.

INTRODUCTION

An insensitive high explosive (IHE) with high safety and high performance is preferred over a sensitive HE. The former differs from the latter not only in initiation characteristics but also in detonation characteristics. An IHE is characterized by (i) the presence of gaseous HF as a detonation product, (ii) a large carbon-content, and (iii) a slow energy release as indicated by a significant detonation front curvature and the diameter-dependence of the detonation velocity. This paper describes items of importance to the IHE detonation: (a) the HF-HF intermolecular potential and those between HF and other detonation products; (b) the effect of fluorine chemistry on supercritical fluid phase change in detonation product mixtures; (c) the kinetics associated with carbon coagulation; (d) a new HE burn model to account for the slow energy release associated with carbon kinetics. We apply the resulting model to produce equations of state (EOS) of IHEs and interpret experimental data of LX-17.

INTERMOLECULAR POTENTIALS INVOLVING HF

A typical IHE such as LX-17 uses a binder containing fluorine atoms. It produces hydrogen fluoride (HF) as a detonation product. Hence, the prediction of performance of an IHE requires information on the intermolecular potentials involving HF. However, because of its highly corrosive character, experimental data of HF (e.g., shock wave) are not available, making it difficult to formulate reliable intermolecular potentials involving HF under detonation condition. As a guide in deriving effective pair potentials between HF and other detonation products (HF, CO_2 , H_2O , NH_3), we use the low-temperature (T) condensed-phase structure of HF and detonation properties of five high explosives containing F atoms: FEFO ($C_5H_6N_4O_{10}F_2$), FM1 ($C_{1.906}H_{2.872}N_{1.265}O_{3.164}F_{0.308}$), PF ($C_6H_2N_3O_6F_1$), LX-17 ($C_{2.295}H_{2.186}N_{2.150}O_{2.150}F_{0.2}$), and 1,2DP ($C_3H_6N_2F_2$). HF molecules have hydrogen-bond strength of about 0.3 eV and form chain- and ring-clusters in the gas and liquid phases. The crystal structure of HF is

orthorhombic with space group C_{2v}^{12} . It consists of zigzag hydrogen bonded F-F chains that are parallel to the [100] plane. The F-F bond distance in the chain is 2.49 Å at 148 K and the nearest neighbor interchain distances are 3.12 to 3.20 Å.

Figure 1 shows these inter- and intra-chain distances of the crystal structure. It also shows three HF-HF potentials (with $\epsilon = \epsilon_0$) represented by an exponential-6 (exp-6) potential,

$$\phi(r) = \frac{\epsilon}{\alpha - 6} \{ 6 \exp[\alpha(1 - r/r^*)] - \alpha(r^*/r)^6 \}, \quad (1)$$

where the well depth ϵ is made temperature-dependent,²

$$\epsilon = \epsilon_0(1 + \lambda/T), \quad (2)$$

to account for the increasingly attractive character of the interaction as the temperature decreases. Equation (1) is a high-temperature correction and is only reliable at $T > \lambda$.

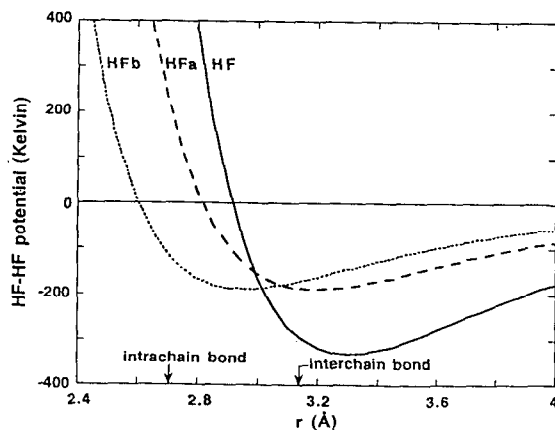


FIGURE 1. PAIR POTENTIALS OF HF. ARROWS INDICATE INTRACHAIN AND INTERCHAIN F-F DISTANCES IN THE HF CRYSTAL.

A HF-HF potential (labeled "HF") was used in our earlier work.¹ Its repulsive range with a potential minimum at r^* ($= 3.30 \text{ \AA}$) $> r_e = 3.12 \text{ \AA}$ (= interchain F-F distance) is too large. Another potential (labeled HFb) has $r^* = 2.95 \text{ \AA}$ ($< r_e$), $\epsilon_0/k = 188.6 \text{ K}$, $\alpha = 13.01$, and $\lambda = 368.6 \text{ K}$. It was obtained using detonation velocities (D_{CJ}) of 1,2DP at the Chapman-Jouguet (CJ) point. Since it gave inconsistent D_{CJ} 's of the other explosives, it has been rejected. The best available potential is labeled HFa ($\epsilon_0/k = 188.6 \text{ K}$, $r^* = 3.19 \text{ \AA}$, $\alpha = 13.01$, $\lambda = 368.6 \text{ K}$). It was obtained by spherically averaging *ab initio* quantum mechanical HF-HF data weighted by a Boltzmann factor.³ Note that r^* ($= 3.19 \text{ \AA}$) of HFa is close to r_e .

Unlike-pair ($i \neq j$) potentials between HF (subscript i) and other detonation products (subscript j) are obtained by using the HFa potential parameters and the generalized Lorentz-Berthelot rule,

$$\epsilon_{ij} = k_{ij} \sqrt{\epsilon_{ii} \epsilon_{jj}}, \quad r_{ij}^* = \frac{1}{2} l_{ij} (r_{ii}^* + r_{jj}^*), \quad (3)$$

$$\alpha_{ij} = m_{ij} \sqrt{\alpha_{ii} \alpha_{jj}},$$

In this work, we set $k_{ij} = m_{ij} = 1$ and determine the values of l_{ij} between HF and detonation products (H_2O , CO_2 , CO), using a Chemical Equilibrium code CHEQ, to match D_{CJ} data of FEFO, LX-04 ($\text{C}_{1.55}\text{H}_{2.58}\text{N}_{2.30}\text{O}_{2.30}\text{F}_{0.52}$), and 1,2DP. The CHEQ code² minimizes the Gibbs free energy of a detonation product mixture with respect to the mole fractions of detonation products, in which the Gibbs free energy of the fluid mixture is computed using exp-6 potentials described above in a statistical mechanical mixture theory.^{2,4} Table 1 gives the resulting values of l_{ij} . Set A is based on an empirical carbon EOS calibrated to the performance of TNT ($\text{C}_7\text{H}_6\text{N}_3\text{O}_5$).¹ Set B which was chosen in actual calculations is based on a model, which allows the carbon cluster growth by diffusion discussed later. Note that the overall determination of the interactions is sensitive to the accuracy and completeness of the experimental data and also to the carbon cluster model. Set A uses $l_{ij} = 1$ for the CO-HF interaction, since the effect on the detonation pressure (P) was too small to offer a good test. Table 2 shows the CJ pressures (P_{CJ}) and D_{CJ} for FEFO and LX-04

TABLE 1. CORRECTION FACTOR l_{ij} , EQ. (3).

	Correction factor	
	l_{ij}	
	Set A	Set B
H ₂ O - HF	1.101	0.976
CO ₂ - HF	0.841	1.095
CO - HF	1.0	1.080

TABLE 2. SENSITIVITY OF D_{CJ} TO LIKE- AND UNLIKE-PAIR POTENTIALS OF HF

Pot-entia	Corr. factor	$D_{CJ}(\text{km/s})$	
		FEFO	LX-04
HFa	Set A	7.40	8.65
HFa	Set B	7.51	8.45
HFb	Set B	7.70	8.67
Experiment		7.50	8.46

obtained by using the HFa or HFb potential together with Set A or Set B for parameter l_{ij} . The differences in the calculated D_{CJ} between the HFa and HFb potentials are about 2.5 % for FEFO and LX-04. These are significant differences. It shows that accurate knowledge of the HF potential is critical to the HE performance prediction.

SUPERCritical FLUID PHASE CHANGES ASSOCIATED WITH FLUORINE CHEMISTRY AND EFFECTS OF HE EOS

Currently available studies on supercritical fluid phase separations are limited to mixtures of chemically nonreactive species. These are not directly relevant to describe the postdetonation products of HEs, which contain chemically reactive systems such as CO , CO_2 , H_2O , N_2 , etc. In addition, our earlier statistical mechanical calculations⁵ revealed that post-detonation mixtures containing C, N, H, O atoms can separate into an N_2 -poor and an N_2 -rich fluid phases (hereafter, referred to as phase α and phase β , respectively.) A binder such as Kel-F or viton A used in the formulation of an IHE contains F atoms. They react with H or C atoms to produce HF and CF_4 . We show below important influence of HF and CF_4 on phases α and β . Such calculations are carried out for LX-17 (TATB with Kel-F binder) and LX-04 (HMX with viton A binder).

Figure 2 shows Hugoniot of LX-17 based on CHEQ, assuming the HE to burn 100% and 96.5%, respectively. Both calculations use the HFa set for the HF-HF potential and Set A (in Table 1) for unlike-pair interactions involving HF. The reason for the two calculations will be elaborated later. We focus here on the 96.5% burn Hugoniot, which shows a 'kink' near 50 GPa. The kink is a manifestation of how the fluorine chemistry complicates the α - β phase separation. Namely, up to about 50 GPa, F atoms form HF molecules and occur in the α phase containing H_2O molecules. This is so, because HF and H_2O are hydrogen bonding molecules and prefer to associate with each other. However, above this (P, T) range, F atoms appear in the β phase as CF_4 molecules, as high

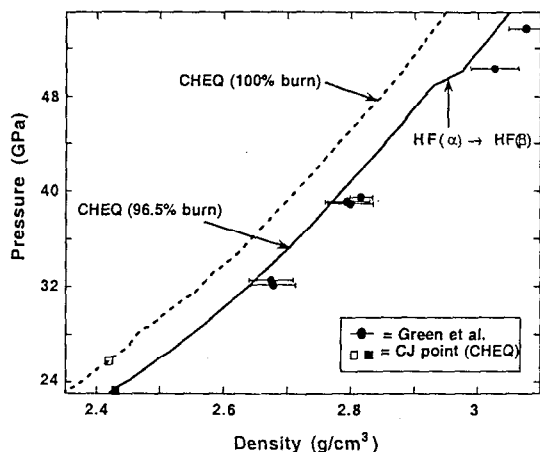


FIGURE 2. CHEQ HUGONIOTS OF LX-17 VS. EXPERIMENT.¹²

pressure forces F atoms to be in a more compact CF_4 structure to reduce the thermodynamic free energy (Le Chaterlier's principle).

Figure 3 highlights this fluorine chemistry by comparing the mole fractions (= moles/total number of moles in a given phase) of N_2 , H_2O , HF, and CF_4 along the 0.5-eV isotherm of LX-04. We note that F atoms alter the α - β phase change at different pressure levels. First, within a small interval (P_1, P_2) indicated by open arrow in Figure 3, the fluid mixture separates into phase α (solid line) which is rich in HF and phase β (dashed line) which is rich in H_2O . At the next interval (P_2, P_3), H_2O molecules gradually change their phase preference from phase β to phase α to be close to HF molecules. But, at $P > P_3$, HF molecules in phase α become thermodynamically unstable with respect to formation of CF_4 molecules, which prefer to be in phase β . This last phase separation is abrupt in a thermodynamic sense and occurs at pressure P_3 that is well above P_1 . Examination of Figure 3 shows that this phase separation involves the formation of diamond through a chemical reaction, $2CO(\beta) + 4HF(\alpha) \rightarrow CF_4(\beta) + 2H_2O(\alpha) + C(\text{diamond})$.

It should be noted that this shift in fluorine chemistry is extremely sensitive to the unlike pair potentials between HF and other species. For example, if Set B is used instead of Set A, the shift in fluorine chemistry, $HF(\alpha) \rightarrow CF_4(\beta)$, is not abrupt and starts gradually from the pressure (P_1) where the N_2 -rich fluid phase separation occurs first.

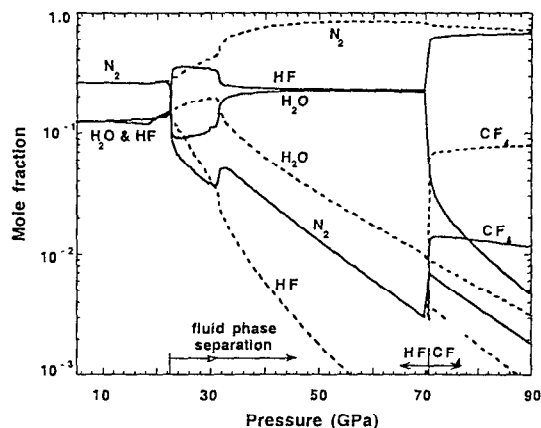


FIGURE 3. MOLE FRACTIONS OF DETONATION PRODUCTS OF LX-04 AT 0.5 eV: SOLID LINE = PHASE α ; DASHED LINE = PHASE β .

CARBON KINETICS

The carbon-rich class of HEs (such as TATB and TNT) is different from other classes of HEs with CHNO atomic composition. In the latter cases, their thermochemistry is dominated by gaseous chemical reactions. Because these reactions are very fast, an assumption of thermochemical equilibrium results in reliable prediction of the HE performance. In contrast, carbon condensation reactions in carbon-rich HEs can take long time (often longer than the time scale of a typical detonation experiment). Hence, the post-detonation EOS of carbon-rich HEs needs to consider both the thermodynamics of chemically reactive mixtures, as well as the kinetics of carbon coagulation.⁶

A detonation wave consists of a compressive and an expansion parts. The former includes (i) the detonation front representing an unreacted HE, (ii) a reaction zone where HE molecules undergo endothermic and exothermic reactions and dissociate, and (iii) a steady state point, where the kinetic energy of reaction products drives the compressive portion ahead of the expansion part of the detonation wave. The resulting steady detonation front travels with the sound speed (relative to the medium) of the following peak rarefaction wave. The CJ theory assumes the steady state to be in thermodynamic equilibrium. In zone (ii), carbon atoms from the dissociation products will start to form clusters by diffusion and grow into larger clusters. If we assume thermodynamic equilibrium, these carbon clusters should be in the diamond phase with sp^3 -bonding. Our analyses⁶ of experimental TNT data indicated that this is true in some instances but not so in other cases. In the latter cases the detonation behavior is consistent with an assumption that carbon clusters form a graphitic solid

with sp^2 -bond. It implies that the final state is not in thermodynamic equilibrium but in a metastable state. It also implies that the CJ theory is not applicable for a carbon-rich HE. The expansion portion of the detonation wave contains the hot gases and carbon clusters left behind. These gases continue to exert pressure and perform most of the work of the explosion. Here, as the pressure drops, the diamond clusters transform back to graphitic clusters. Hence, our modeling effort must also consider the carbon kinetics associated with the expansion portion of the detonation wave.

We consider the coagulation kinetics of carbon clusters by employing the Shaw and Johnson model,⁷ which describes a change in concentration c_k of k -atom clusters by using Smoluchowski equations; i.e.,

$$dc_k/dt = \sum_{i+j=k} k_{ij} c_i c_j - 2c_k \sum_j k_{jk} c_j, \quad (4)$$

where $k_{ij} \equiv 4\pi(D_i + D_j)R_{ij}$ (D_i = diffusion constant of a cluster with i atoms; R_{ij} = collision diameter between clusters of sizes i and j). Shaw and Johnson derived an approximate analytic solution for Eq. (4),

$$c_k = n_0 [x/(1+x)]^{k-1} / (1+x)^2, \quad (5)$$

in terms of the initial carbon concentration n_0 and a dimensionless time x ,

$$x \equiv 4\pi DR t n_0 = (2kT/3\eta) t n_0, \quad (6)$$

where $D_i R_i = \text{constant} = DR$. The second equality in Eq. (6) results from the Stokes-Einstein equation relating DR to the viscosity η of the medium.

The surface energy correction $\langle \Delta E \rangle$ to the bulk carbon energy is obtained by averaging the surface energy of k -atom cluster $\Delta E_k \approx Ak^{2/3}$ over c_k ; i.e.,

$$\Delta \bar{E} \approx A \Gamma(5/3) / [x + \Gamma(5/3)]^{1/3}. \quad (7)$$

We implemented Eqs. (6) and (7) in the CHEQ code by approximating the surface corrections to the Helmholtz free energy for graphite and diamond, $\Delta A_{\text{graphite}} \approx \langle \Delta E_{\text{graphite}} \rangle$ and $\Delta A_{\text{diamond}} \approx \langle \Delta E_{\text{diamond}} \rangle$. The viscosity η is given by the modified Enskog theory,⁸

$$\eta = \eta_0 (2\pi/3) \rho d^3 [Y - 1 + 0.8 + 0.761Y], \quad (8)$$

$$\eta_0 = (5/16\pi d^2) (\pi m k T)^{1/2}, \quad (9)$$

where $Y = \beta P/\rho - 1$. Equations (8) and (9) require information on the hard-sphere diameter d and the mass m of the medium. The CHEQ code provides d through

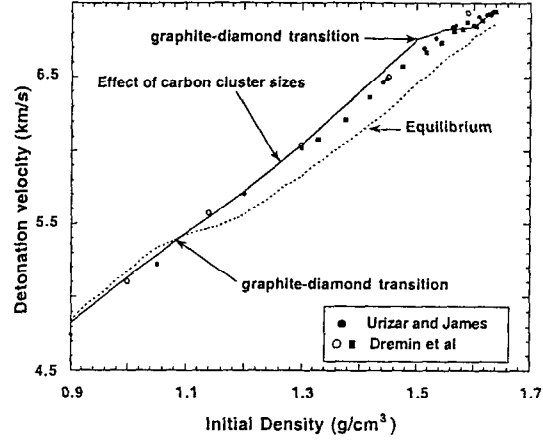


FIGURE 4. D_{CJ} VS. ρ_0 OF TNT: CHEQ VS. EXPERIMENT.^{10,11}

the effective one-component mixture formulation. A similar effective one-component mass m is available,⁹

$$\frac{1}{m} = \frac{\sum_i \sum_j x_i x_j \epsilon_{ij} r_{ij}^* / m_j}{\sum_i \sum_j x_i x_j \epsilon_{ij} r_{ij}^*}, \quad (10)$$

where r_{ij}^* and ϵ_{ij} are parameters for exp-6 potentials between species i and j , and m_j is the mass of species j . In Eq. (10) a set $\{x_i\}$ represents the composition of detonation products, as determined in CHEQ by minimizing the Gibbs free energy with respect to x_i .

Figure 4 illustrates effects of the graphite-diamond phase change on D_{CJ} of TNT with different initial densities ρ_0 . The calculation was done at fixed time (= 150 ns) behind the detonation front. This time interval is a typical reaction zone thickness for TNT. The lower curve assumes thermodynamic equilibrium. The upper curve is obtained from the carbon kinetics model by adjusting $A_{\text{diamond}} = 70$ kcal/mol and using $A_{\text{graphite}} = 40.94$ kcal/mol. It raises the transition pressure (hence, D_{CJ}) and, thereby, make the theoretical prediction agree closer to experiment.^{10,11} At low ρ_0 , the graphite-to-diamond conversion rate is slow because of low pressure and temperature conditions. Consideration of the surface energy causes these clusters to be graphitic with sp^2 -like bonding as opposed to diamond with sp^3 -like bonding. At high ρ_0 , the diffusion and conversion rates are fast, enabling carbon clusters to grow larger and making diamond-like clusters become thermodynamically favorable. The kink in D_{CJ} at $\rho_0 = 1.5$ g/cm³ in Figure 4 signifies the graphite-to-diamond

transition so that diamond clusters become stable above the kink.

NEW HE BURN MODEL WITH THE DIFFUSION LIMITED CARBON KINETICS

Another important physics issue is an indication that available IHEs tend to burn slowly or incompletely, as mentioned in connection with Figure 2, which clearly shows the CHEQ equilibrium Hugoniot of LX-17 to be stiffer than experiment.¹² A 3.5% reduction in the amount of burn brings the theory closer to experiment. It implies that the HE has not fully reacted. Not shown are the CJ expansion adiabat below the CJ point. A 3.5% reduction in the amount of the HE also offers good agreement there. A complete description of such kinetics is far more complex than the nonequilibrium description given above. It requires a hydrodynamic study with constitutive relations as well as initial and boundary conditions. The model presented below represents a compromise between the need to capture the physics of the carbon cluster kinetics with as much detail as possible and the need to minimize the computational work involved, such that a hydrodynamic calculation can be completed in a reasonable time.

The dimensionless time variable x defined by Eq. (6) is independent of the cluster size but depends on the local temperature and viscosity of the detonation product gases. Shaw and Johnson assumed constant thermodynamic and transport properties, whereas physically these quantities change over the duration of a hydrodynamic process. However, Eq. (5) is still valid for the case of a time-varying temperature and viscosity if x in Eq. (5) is replaced with an integrated dimensionless time variable,

$$\tau = \int_{t_{burn}}^t 4\pi DR[\rho(t), e(t)] n_0 dt. \quad (11)$$

In Lagrangean hydrodynamic calculations, it means that we need to keep a running integral, Eq. (11), for each Lagrange zone. The release of cluster surface energy can be calculated by replacing x with τ in Eq. (6); i.e., $\langle \Delta E \rangle \approx A \Gamma(5/3)/[\tau + \Gamma(5/3)]^{1/3}$. A decrease in $\langle \Delta E \rangle$ due to the cluster growth is balanced by a corresponding increase in the thermal energy of the carbon clusters. The delayed energy release from the cluster growth in a Lagrange zone should then appear as an increment in the hydrodynamic internal energy of the zone.

The standard β burn model¹³ is usually used to simulate a detonation front in hydrodynamic calculations. It is described by a burn fraction f

multiplying the pressure P_{eq} representing the detonation product EOS,

$$P = f P_{eq}(\rho, e), f = \min[1, \beta(1 - \rho_0/\max[\rho])]. \quad (12)$$

The initial conditions within the unburned explosive are taken to be

$$P = 0, e = e_0, \rho = \rho_0, f = 0, \quad (13)$$

where e_0 is the chemical energy released by the burning of HE and ρ_0 is its initial unburned density.

In the case where all of the chemical energy is released in a thin reaction zone, β is chosen so that f approaches 1 as ρ approaches the density specified by the CJ theory. It needs to be emphasized that a hydrodynamic integration knows about the CJ theory only though this particular choice of β . Otherwise, a range of possible detonation velocities (D), densities, and pressures can be obtained by using different choices of β . Given the initial state Eq. (13), alternate hydrodynamic solutions, consistent with conservation of mass, momentum, and energy across the detonation front, can be obtained introducing a parameter f_{fast} :

$$f = f_{fast}, \rho = \frac{\beta \rho_0}{\beta - f_{fast}}, D = \sqrt{\frac{\beta P}{\rho_0 f_{fast}}} \quad (14)$$

$$P = f_{fast} P_{eos} \left[\frac{\beta \rho_0}{\beta - f_{fast}}, e_0 + \frac{P f_{fast}}{2\beta} \right].$$

These properties suggest that the modified β burn model Eq. (14) can be adapted to model the fast gas reaction zone in a burn front followed by a slow diffusion limited release of the remaining energy.

Such a model can be constructed by introducing the fast and slow reaction zones which are joined at the point where f has increased to an input fraction f_{fast} , corresponding the fraction of the energy released by the fast gas reactions. Then, f can be allowed to relax to 1, following a $\tau^{-1/3}$ -decay,

$$f = \min[f_{fast}, \beta(1 - \rho_0/\max[\rho])], f < f_{fast}, \quad (15a)$$

$$f = 1 + (f_{fast} - 1)(\tau_{fast}/\tau)^{1/3}, f \geq f_{fast}. \quad (15b)$$

The time t_{burn} in Eq. (11) is defined as the time at which f first departs from 0, so that τ reaches τ_{fast} by the time f reaches f_{fast} . Because the time scaling factor $1/DRn_0$ is so short relative to hydrodynamic times, τ typically is in the range of 10^4 to 10^5 by the time f reaches f_{fast} . A

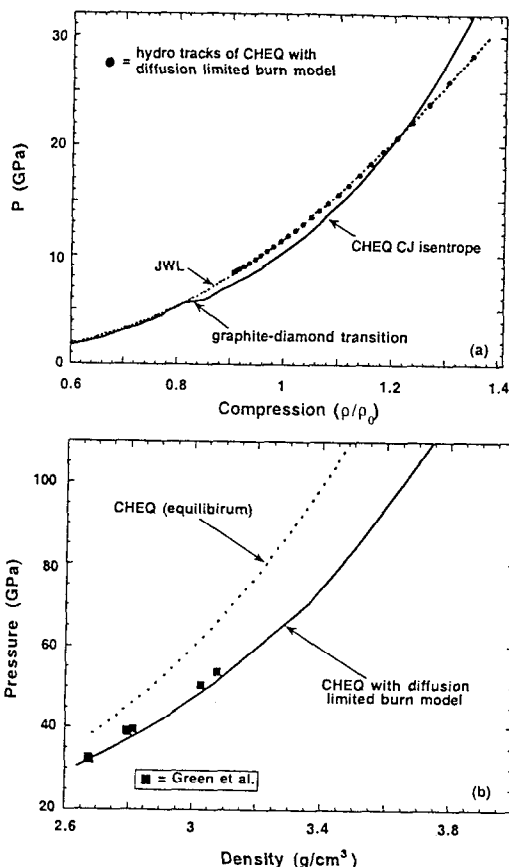


FIGURE 5. LX-17: (a) EXPANSION TRACK OF HYDRO VS. CHEQ CJ ISENTROPE AND CYLINDER/JWL; (b) HUGONIOT: HYDRO SIMULATIONS VS. EXPERIMENT.¹²

smooth switch from β burn growth Eq. (15a) to diffusion limited growth Eq. (15b) can be obtained by setting τ_{fast} to the τ calculated in each Lagrange zone at the time f reaches f_{fast} in each zone.

HYDRODYNAMIC APPLICATIONS

As mentioned earlier, measured detonation velocities of LX-17 tend to be roughly 10% below what is predicted by the CJ theory. In the context of the modified β burn model described above, a lower detonation velocity can be obtained by reducing β and f_{fast} , although this also changes the density and pressure behind the fast burn front. However, given a slow delayed release of the detonation energy, the use of the CJ theory to determine β is not justified. Under these conditions an alternative is to use the

conservation conditions Eq. (14) to select a β that yields a hydrodynamic burn velocity consistent with measured detonation velocities. That not all of the chemical energy in LX-17 is released in the fast reaction zone suggests that the increase in f with ρ specified in Eq. (12), should be limited to f_{fast} that is less than 1. With these modifications to the β burn model, the effective energy release across the fast reaction burn front can be limited while maintaining a propagation velocity consistent with measured values.

Equation (7) has an asymptotic time decay of $\tau^{1/3}$. This corresponds to a rapid initial decay following the fast gas reactions with a subsequent slow asymptotic relaxation to the zero surface energy of bulk carbon. The magnitude of $1/DRn_0$ is about 10^{-12} seconds, so that the $\tau^{1/3}$ dependence is relevant to the time scales of a typical hydrodynamic integration.

Figure 5a shows a comparison of a hydrodynamic expansion track of a Lagrangean zone in a one-dimensional burn of an infinite slab of LX-17 and the cylinder tests (LH-JWL)¹³ track. The calculation was done in CHEQ with diffusion limited carbon kinetics. The CHEQ CJ isentrope is also shown for comparison. Figure 5b shows the Hugoniot of LX-17 obtained from a series of hydrodynamic simulations of a plane detonation front driven by a piston moving at constant speeds, ranging from 1.5 to 3 km/s. Also shown are experimental data by Green et al.,¹² and the CHEQ equilibrium Hugoniot using the bulk carbon EOS. Slowing down the release of the detonation energy reduces the detonation velocity, and increases the density of the detonation product gases. Although the diffusion limited burn model is highly simplified, it improves agreement between theory and experiment. These simulations of a self-sustaining detonation wave in LX-17 predict the steady state at $(\rho_s, P_s, D_s) = (2.67 \text{ g/cm}^3, 32.0 \text{ GPa}, 7.60 \text{ km/s})$ compared to the cylinder-test values $(2.62 \text{ g/cm}^3, 30.0 \text{ GPa}, 7.60 \text{ km/s})$, while the equilibrium CHEQ predicts $(2.42 \text{ g/cm}^3, 27.3 \text{ GPa}, 8.23 \text{ km/s})$ at the CJ point.

We are now testing the CHEQ/carbon diffusion kinetics using the LX-17 data from a "bigplate" experiment described by Souers et al.^{13,14} This experiment consists of a HE disk, 100 mm in radius and 40 mm thick. Detonation at the center of the backside sends an expanding detonation wave, which pushes a 0.5 mm-thick Cu plate that is glued to the front side of the HE. The plate velocity is measured by a Fabry-Perot interferometer focused at different radial positions.

Figure 6 shows 'on-center' comparisons at center of the Cu plate between spherically symmetric one-dimensional (KO) hydrodynamic¹⁵ simulations and

Fabry data, as recently reported by Souers et al.¹⁴ These data (with estimated uncertainties of $\pm 0.1 \mu\text{s}$) are in good agreement with one of our most detailed calculations, referred to as 'Standard set' to about $0.4 \mu\text{s}$. This calculation uses a high resolution HE zone (0.02 mm), the detonation model with carbon coagulation kinetics, the Cochran-Banner spall model, and the Steinberg-Guinan strength model. The other calculations represent effects of individually relaxing these hydro/physics constraints. Figure 6 clearly shows importance of the carbon diffusion kinetics. The program burn model fails to approach the compression needed at the CJ conditions. The use of a coarser zone (0.1 mm) smears out the early velocity-time record. All these factors cause the calculations to underestimate the initial Cu plate jump-off velocities. Exclusion of the spall or material strengths (not shown) produces the oscillatory behavior of the plate velocity that differs significantly from experiment.

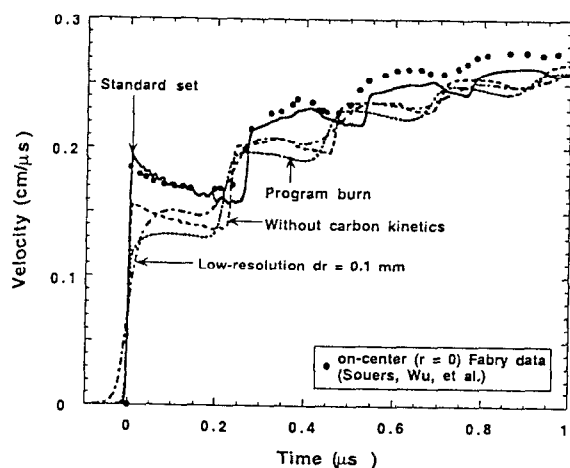


FIGURE 6. Cu BIGPLATE DRIVEN BY LX-17: 1-D HYDRO RUNS WITH CHEQ EOS VS. EXPERIMENT.^{13,14}

The new HE burn model described here does not include the portion of the spike pressure decay associated with the prompt reaction zone, since we use an artificial viscosity coupled with β -burn to model the lead shock and prompt reaction zone. Although the mesh used in the calculations can be made small enough to correspond to a physically reasonable prompt burn zone, this is an additional source of uncertainty in the model. Hugoniot data for unburned LX-17 suggest that the error in the calculated maximum spike pressure due to these approximations is of the order of 5%.

The late-time deviations in Fig. 6 could come from possible interactions with off-center hydro-zones

which our 1-D calculations did not include. Or, it could be due to a reverse transformation of diamond clusters into graphitic clusters as pressure drops behind the detonation front. A nonequilibrium CHEQ calculation, including carbon kinetics, shows that the reverse reaction can indeed raise the detonation pressure from the equilibrium value. One can examine the issues discussed here in detail by implementing the relevant kinetics and CHEQ directly into a two-dimensional hydro code.

CONCLUDING REMARK

Unlike a sensitive HE, CHEQ calculations on an IHE do not give uniformly good comparisons with experiment. This paper has presented detailed models dealing with two physics factors that are responsible for it; i.e., uncertainties in interaction potentials involving F atoms and a need to model the kinetics of carbon clusters during condensation processes. The former is an equilibrium effect; the latter a kinetics effect. Without a satisfactory description of the former, we can not expect to achieve a proper prediction of the HE performance, including the carbon kinetics or any kinetics effect for that matter.

In this regard, F atoms appear mostly as HF in a fluid phase α (poor in N_2) up to a certain pressure level, beyond which they start to form CF_4 in a fluid phase β (rich in N_2). This shift in fluorine chemistry, $\text{HF}(\alpha) \rightarrow \text{CF}_4(\beta)$, can be abrupt or gradual in pressure and is extremely sensitive to small variations in the unlike pair potentials between HF and other detonation products. It can significantly affect the computed Hugoniot of LX-17 and LX-04. The change in fluorine chemistry can occur at pressure as low as 10 to 20 GPa at 1000 K. This range is accessible by present-day high-pressure experiment.

This paper described the first of the two steps involved in the carbon kinetics; i.e., diffusive coagulation of carbon clusters (and its implementation in CHEQ). The next step is the kinetics of the graphite-diamond transition, which occurs when graphitic clusters grow so large that surface effects favoring the graphitic form become no longer important, making graphitic clusters energetically less favorable over the formation of diamond-like clusters. Similarly, diamond clusters behind the detonation wave undergo a reverse transformation along the expansion path, as the pressure drops. In both cases the presence of an energy barrier between graphitic and diamond clusters will kinetically limit the transformation process. There is no a priori reason to favor the diffusion kinetics over the solid-phase transformation kinetics. We are presently investigating this solid-phase transformation kinetics.

This paper also presented a HE burn model with cluster diffusion kinetics and its implementation in one- and two-dimensional hydrodynamic codes. Resulting calculations have shown significantly improved agreement with experiment. We have incorporated CHEQ directly into the one-dimensional hydrocode. A similar effort to do it in the two-dimensional hydrocode is in progress. Such an 'on the fly' CHEQ/hydro code is needed to examine the reverse kinetics involving the diamond to graphite transformation. With this coupled hydrocode-CHEQ model, we also plan to examine other kinetic processes which may affect the performance of IHEs.

ACKNOWLEDGMENT

This work was done under the auspices of the U.S. Department of Energy by the Lawrence Livermore National Laboratory under contract number W-7405-ENG-48 and funded by the Accelerated Strategic Computing Initiative (ASCI). We thank Drs. Clark Souers and Ben Wu for providing a draft of Ref. 14 to us prior to its publication.

REFERENCES

1. Van Thiel, M., Ree, F. H., and Haselman, L. C., "Accurate Determination of Pair Potentials for a $C_wH_xN_yO_z$ System of Molecules: A Semiempirical Method," Report UCRL-ID-120096 (Lawrence Livermore Laboratory, 1995).
2. Ree, F. H., "A Statistical Mechanical Theory of Chemically Reacting Multiphase Mixtures: Application to the Detonation Properties of PETN," *J. Chem. Phys.*, **81**, 1984, pp. 1251-1263.
3. Ree, F. H., and Calef, D. F., "Theoretical Hugoniot of Liquid Hydrogen Fluoride," in *Shock Compression of Condensed Matter-1989*, Eds. S. C. Schmidt, J. N. Johnson, and L. W. Davison (Elsevier Science, NY, 1990) pp. 87-90.
4. F. H. Ree, "Simple Mixing Rule for Mixtures with EXP-6 Interactions," *J. Chem. Phys.*, **78**, 1983, pp. 409-415.
5. F. H. Ree, "Supercritical Fluid Phase Separations: Implications for Detonation Properties of Condensed Explosives," *J. Chem. Phys.*, **84**, 1986, pp. 5845-5856.
6. Van Thiel, M. and Ree, F. H., "Properties of Carbon Clusters in TNT Detonation Products: The Graphite Diamond Transition," *J. Appl. Phys.*, **62**, 1987, pp. 1761-1767.
7. Shaw, M. S. and Johnson, J. D., "Carbon Clustering in Detonations," *J. Appl. Phys.* **62**, 1987, pp. 2080-2085.
8. McQuarrie, D., *Statistical Mechanics* (Harper & Row, New York, 1976), p. 441.
9. Ree, F. H., "Solubility of H_2 -He Mixtures in Fluid Phases to 1 GPa," *J. Phys. Chem.*, **87**, 1982, pp. 2846-2852.
10. Urizar, M. J., James, Jr., E. and Smith, L. C., "Detonation Velocity of Pressed TNT," *Phys. Fluids*, **4**, 1960, pp. 262-274.
11. Dremin, A. N. and Pokhil, P. F., "The Detonation Wave Parameters of Trotyl, Hexogen, Nitroglycerin and Nitromethane," *Proc. Acad. Sci. USSR Phys. Chem. Sec.* **128** (1959) pp. 839-841; Dremin, A. N., Pershin, S. V., Pyaterev, S. V. and Tsaplin, D. N., "Discontinuity in the Relation between the Speed of Detonation Wave and the Initial Density of TNT," *Combustion, Explosion, and Shock Waves*, **25**, 1990, pp. 649-652.
12. Green, L., Lee, E., Mitchell, A., and Tarver, C., "The Supra Compression of LX-04, LX-17, PBX-9404, and RX-26-AF and The Equations of State of The Detonation Products," in *Proc. Eighth Symposium (International) on Detonation*, Albuquerque, NM July 1985, NSWC MP 86-194, (Naval Surface Weapons Center, White Oak, Silver Spring, MD 20903-5000, 1986) pp. 587-595.
13. Souers, P. C., Wu, B. and Haselman, Jr., L. C., "Detonation Equation of State at LLNL, 1995," Report UCRD-ID-119262 Rev. 3 (Lawrence Livermore National Laboratory, 1996), p. 1-11.
14. Souers, P. C., Anderson, S., Avara, R., Fried, L., Janzen, J., McGuire, S., and Wu, B., "Bigplate: An Oblique Angle Explosive EOS Test," UCRL-ID-131282, (Lawrence Livermore Laboratory, 1998).
15. Wilkins, M. L., "Calculation of Elastic-Plastic Flow" in *Methods in Computational Physics*, Vol. 3, Eds. Alder, B., Fernbach, S., Rotenberg M., (Academic Press, 1964), pp. 211-263.